

Iteratively Coupled Multiple Instance Learning from Instance to Bag Classifier for Whole Slide Image Classification

Hongyi Wang¹, Luyang Luo², Fang Wang³, Ruofeng Tong^{1,4}
Yen-Wei Chen^{1,4,5}, Hongjie Hu³, Lanfen Lin¹, and Hao Chen^{2,6} (✉)

¹ College of Computer Science and Technology, Zhejiang University, Hangzhou, China

² Department of Computer Science and Engineering, The Hong Kong University of Science and Technology, Hong Kong, China

³ Department of Radiology, Sir Run Run Shaw Hospital, Hangzhou, China

⁴ Research Center for Healthcare Data Science, Zhejiang Lab, Hangzhou, China

⁵ College of Information Science and Engineering, Ritsumeikan University, Kusatsu, Japan

⁶ Department of Chemical and Biological Engineering, The Hong Kong University of Science and Technology, Hong Kong, China
jhc@cse.ust.hk

Abstract. Whole Slide Image (WSI) classification remains a challenge due to their extremely high resolution and the absence of fine-grained labels. Presently, WSIs are usually classified as a Multiple Instance Learning (MIL) problem when only slide-level labels are available. MIL methods involve a patch embedding process and a bag-level classification process, but they are prohibitively expensive to be trained end-to-end. Therefore, existing methods usually train them separately, or directly skip the training of the embedder. Such schemes hinder the patch embedder’s access to slide-level labels, resulting in inconsistencies within the entire MIL pipeline. To overcome this issue, we propose a novel framework called Iteratively Coupled MIL (ICMIL), which bridges the loss back-propagation process from the bag-level classifier to the patch embedder. In ICMIL, we use category information in the bag-level classifier to guide the patch-level fine-tuning of the patch feature extractor. The refined embedder then generates better instance representations for achieving a more accurate bag-level classifier. By coupling the patch embedder and bag classifier at a low cost, our proposed framework enables information exchange between the two processes, benefiting the entire MIL classification model. We tested our framework on two datasets using three different backbones, and our experimental results demonstrate consistent performance improvements over state-of-the-art MIL methods. Code will be made available upon acceptance.

Keywords: Multiple Instance Learning · Whole Slide Image · Deep Learning.

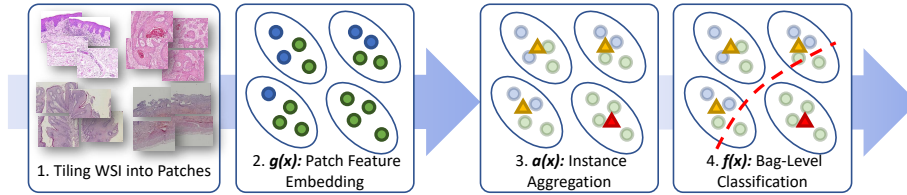


Fig. 1. The typical pipeline of traditional MIL methods on WSIs.

1 Introduction

Whole slide scanning is increasingly used in disease diagnosis and pathological research to visualize tissue samples. Compared to traditional microscope-based observation, whole slide scanning converts glass slides into gigapixel digital images that can be conveniently stored and analyzed. However, the high resolution of WSIs also makes their automated classification challenging [13]. Patch-based classification is a common solution to this problem [7, 22, 2]. It predicts the slide-level label by first predicting the labels of small, tiled patches in a WSI. This approach allows for the direct application of existing image classification models, but requires additional patch-level labeling. Unfortunately, patch-level labeling by histopathology experts is expensive and time-consuming. Therefore, many weakly-supervised [7, 22] and semi-supervised [4, 2] methods have been proposed to generate patch-level pseudo labels at a lower cost. However, the lack of reliable supervision directly hinders the performance of these methods, and serious class-imbalance problems could arise, as tumor patches may only account for a small portion of the entire WSI [10].

In contrast, MIL-based methods have become increasingly preferred due to their only demand for slide-level labels [16]. The typical pipeline of MIL methods is shown in Fig. 1, where WSIs are treated as bags, and tiled patches are considered as instances. The aim is to predict whether there are positive instances, such as tumor patches, in a bag, and if so, the bag is considered positive as well. In practice, the large number of image patch instances requires a fixed ImageNet pre-trained feature extractor $g(x)$ to convert them into feature maps due to limited GPU memory. These instance features are then aggregated by $a(x)$ into a slide-level feature vector to be sent to the bag-level classifier $f(x)$ for MIL training. Due to the high computational cost, end-to-end training of the feature extractor and bag classifier is prohibitive, especially for high-resolution WSIs. As a result, many methods focus solely on improving $a(x)$ and $f(x)$, leaving $g(x)$ untrained on the WSI dataset (as shown in Fig. 2(b)). However, the domain shift between WSI and natural images may lead to sub-optimal representations, so recently there have been methods proposed to fine-tune $g(x)$ using self-supervised techniques [19, 10, 3] or weakly-supervised techniques [11, 21] (as shown in Fig. 2(c)). Nevertheless, since these two processes are still trained separately with different supervision signals, they lack joint optimization and may still lead to inconsistencies within the entire MIL pipeline.

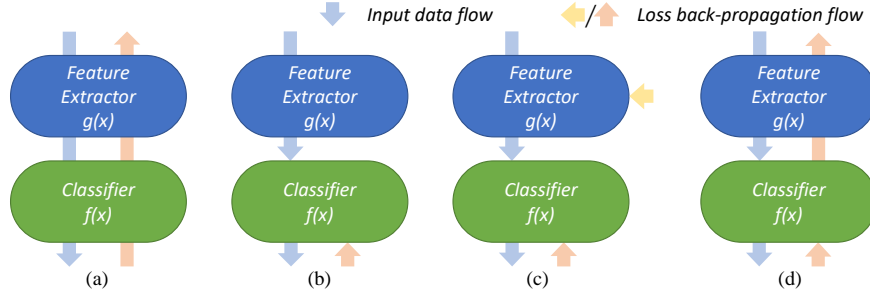


Fig. 2. Comparison between ICMIL and existing methods. (a) Ordinary end-to-end classification pipeline. (b) MIL methods that use fixed pretrained ResNet50 as $g(x)$. (c) MIL methods that introduce extra self-supervised fine-tuning of $g(x)$. (d) Our proposed ICMIL which can bridge the loss back-propagation process from $f(x)$ to $g(x)$ by iteratively coupling them during training.

To address the challenges mentioned above, we propose a novel MIL framework called ICMIL, which can iteratively couple the patch feature embedding process with the bag-level classification process to enhance the effectiveness of MIL training (as illustrated in Fig. 2(d)). Unlike previous works that mainly focused on designing sophisticated instance aggregators $a(x)$ [10,18,12] and bag classifiers $f(x)$ [8,14,23], we aim to bridge the loss back-propagation process from $f(x)$ to $g(x)$ to improve $g(x)$'s ability to perceive slide-level labels. Specifically, we propose to use the bag-level classifier $f(x)$ to initialize an instance-level classifier $f'(x)$, enabling $f(x)$ to use the category knowledge learned from bag-level features to determine each instance's category. In this regard, we further propose a teacher-student [6] approach to generate pseudo labels effectively and fine-tune $g(x)$ simultaneously. After fine-tuning, the domain shift problem is alleviated in $g(x)$, leading to better patch representations. The new representations can be used to train a better bag-level classifier in return for the next round of iteration.

In summary, our contributions are: (1) We propose ICMIL which bridges the loss propagation from the bag classifier to the patch embedder by iteratively coupling them during training. This framework fine-tunes the patch embedder based on the bag-level classifier, and the refined embeddings, in turn, help train a more accurate bag-level classifier. (2) We propose a teacher-student approach to achieve effective and robust knowledge transfer from the bag-level classifier $f(x)$ to the instance-level representation embedder $g(x)$. (3) We conduct extensive experiments on two datasets using three different backbones and demonstrate the effectiveness of our proposed framework.

2 Methodology

2.1 Iterative Coupling of Embedder and Bag Classifier in ICMIL

The general idea of ICMIL is shown in Fig. 3, which follows an Expectation-Maximization (EM) pattern. EM has been used with MIL in some previous

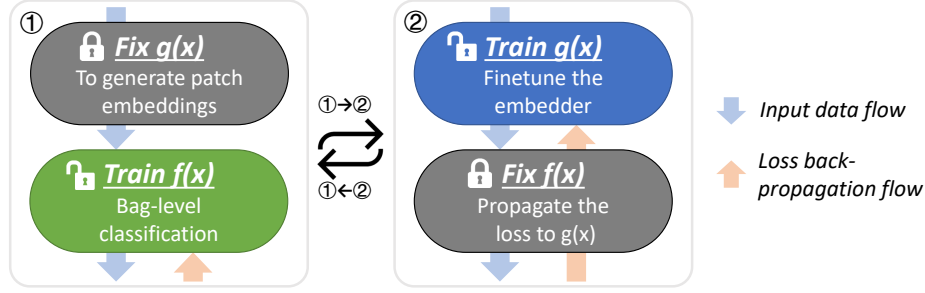


Fig. 3. The core idea of ICMIL: iteratively, ① fix the embedder $g(x)$ and train the bag classifier $f(x)$, ② fix the classifier $f(x)$ and fine-tune the instance embedder $g(x)$.

works [15,11,20], but it was only treated as an assisting tool for aiding the training of either $g(x)$ or $f(x)$ in the traditional MIL pipelines. In contrast, we are the first to consider the optimization of the entire MIL pipeline as an EM alike problem, utilizing EM for coupling $g(x)$ and $f(x)$ together iteratively. To begin with, we first employ a traditional approach to train a bag-level classifier $f(x)$ on a given dataset, with patch embeddings generated by a fixed ResNet50 [5] pre-trained on ImageNet [17] (step ① in Fig.3). Subsequently, this $f(x)$ is considered as the initialization of a hidden instance classifier $f'(x)$, generating pseudo-labels for each instance-level representation. This operation is feasible when the bag-level representations aggregated by $a(x)$ are in the same hidden space as the instance representations'. Luckily, most aggregation methods (e.g., max pooling, attention-based) satisfy this condition since they essentially make linear combinations of instance-level representations.

Next, we freeze the weights of $f(x)$ and fine-tune $g(x)$ with the generated pseudo-labels (step ② in Fig. 3), of which the detailed implementation is presented in Section 2.3. After this, $g(x)$ is fine-tuned for the specific WSI dataset, which allows it to generate improved representations for each instance, thereby enhancing the performance of $f(x)$. Moreover, with the better $f(x)$, we can use the iterative coupling technique again, resulting in further performance gains and mitigation to the distribution inconsistencies between instance- and bag-level embeddings.

2.2 Instance Aggregation Method in ICMIL

Although most instance aggregators are compatible with ICMIL, they still have an impact on the efficiency and effectiveness of ICMIL. Besides that $a(x)$ has to project the bag representations to the same hidden space as the instance representations', it also should avoid being over-complicated. Otherwise, $a(x)$ may lead to larger difference between the decision boundaries of bag-level classifier $f(x)$ and instance-level classifier $f'(x)$, which may cause ICMIL taking more time to converge.

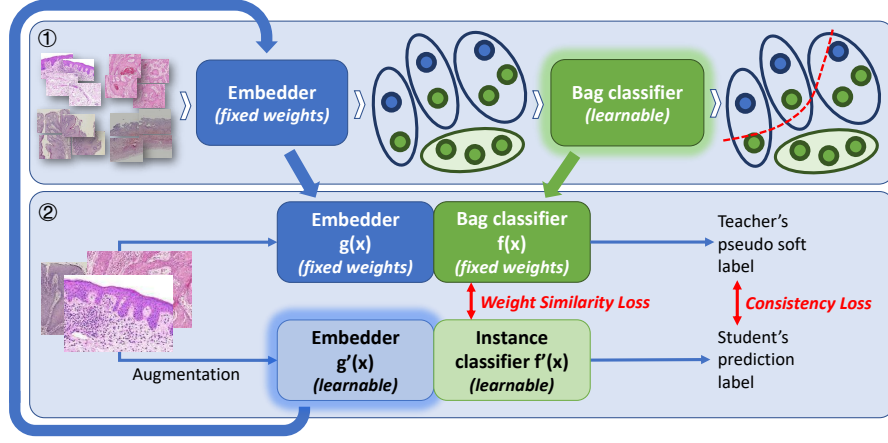


Fig. 4. A schematic view of the proposed teacher-student alike model for label propagation from $f(x)$ to $g(x)$ (mainly in step ②), and its position in ICMIL pipeline.

Therefore, in our experiments, we choose to use the attention-based instance aggregation method [8] which has been widely used in many of the existing MIL frameworks [8,14,23]. For a bag that contains K instances, attention-based aggregation method firstly learns an attention score for each instance. Then, the aggregated bag-level representation H is defined as:

$$H = \sum_{k=1}^K a_k h_k, \quad (1)$$

$$a_k = \frac{\exp\{\omega^T(\tanh(V_1 h_k) \odot \text{sigm}(V_2 h_k))\}}{\sum_{j=1}^K \exp\{\omega^T(\tanh(V_1 h_j) \odot \text{sigm}(V_2 h_j))\}}, \quad (2)$$

where a_k is the attention score for the k -th instance h_k in the bag, ω , V_1 and V_2 are learnable matrices, \odot is element-wise multiplication, and $\tanh()$ and $\text{sigm}()$ are different activation functions. Obviously, H and h_k remains in the same hidden space, satisfying the prerequisite of ICMIL.

2.3 Label Propagation from Bag Classifier to Embedder

We propose a novel teacher-student model for accurate and robust label propagation from $f(x)$ to $g(x)$. The model's architecture is depicted in Fig. 4. In contrast to the conventional approach of generating all pseudo labels and re-training $g(x)$ from scratch, our proposed method can simultaneously process the pseudo label generation and $g(x)$ fine-tuning tasks, making it more flexible. Moreover, incorporating augmented inputs in the training process allows for the better utilization of supervision signals, resulting in a more robust $g(x)$. We

also introduce a learnable $f'(x)$ to self-adaptively modifying the instance-level decision boundary for more effective fine-tuning of the embedder.

Specifically, we freeze the weights of $g(x)$ and $f(x)$ and set them as the teacher. We then train a student patch embedding network, $g'(x)$, to learn category knowledge from the teacher. For a given patch input, the teacher generates the corresponding pseudo label, while the student receives an augmented image x' and attempts to generate a similar prediction to that of the teacher through a consistency loss L_c . L_c is defined as:

$$L_c = \sum_{c=0}^C \left[f(x)_c \log \left(\frac{f(x)_c}{f'(x')_c} \right) \right], \quad (3)$$

where $f(x)$ and $f'(x)$ are teacher classifier and student classifier respectively, and $f(x)_c$ indicates the c -th channel of $f(x)$.

Additionally, during training, a learnable instance-level classifier is used on student to back-propagate gradients to $g'(x)$. The initial weights of $f'(x)$ are the same as those of $f(x)$, as the differences in the instance- and bag-level classification boundaries is expected to be minor. To make $f'(x)$ not so different from $f(x)$ during training, a weight similarity loss, L_w , is imposed to constrain it. By doing so, the patch embeddings from $g'(x)$ can still suit the bag-level classification task well, rather than being tailored solely for the instance-level classifier $f'(x)$. L_w is defined as:

$$L_w = \sum_{l=0}^L \sum_{c=0}^C \left[f(x)_c^l \log \left(\frac{f(x)_c^l}{f'(x)_c^l} \right) \right], \quad (4)$$

where $f(x)_c^l$ indicates the c -th channel of l -th layer's output in $f(x)$. The overall loss function for this step is $L_c + \alpha L_w$, with α set to 0.5 in our experiments.

3 Experiments

3.1 Datasets

Our experiments utilized two datasets, with the first being the publicly available breast cancer dataset, Camelyon16 [1]. This dataset consists of a total of 399 WSIs, with 159 normal and 111 tumour WSIs for the training set, and the remaining 129 for test. While patch-level labels are officially provided in Camelyon16, they are not used in our experiments.

The second dataset is a private hepatocellular carcinoma (HCC) dataset collected from Hangzhou Sir Run Run Shaw Hospital. This dataset comprises a total of 1140 valid tumor WSIs scanned at $40\times$ magnification, and the objective is to identify the severity of each case based on the Edmondson-Steiner (ES) grading. The ground truth labels are binary classes of low risk and high risk, which are provided by experienced pathologists.

Table 1. Results of ablation studies on Camelyon16 with AB-MIL.

(a) Ablation study on the ICMIL iteration times								(b) Loss Propagation		
ICMIL Iterations	0	0.5	1	1.5	2	2.5	3	Method	Naïve	Ours
AUC	85.4	88.8	90.0	89.7	90.5	90.4	90.0	AUC	88.5	90.0
F1	78.0	79.4	80.5	80.1	82.0	80.7	81.7	F1	78.8	80.5
Acc	84.5	85.0	86.6	86.0	85.8	86.9	86.6	Acc	83.9	86.6

Table 2. Comparison with other methods on Camelyon16 and HCC datasets. Best results are in bold, while the second best ones are underlined.

Method	Loss Propagation			Camelyon16			HCC		
	$g(x)$	$f(x)$	$f \rightarrow g$	AUC(%)	F1(%)	Acc(%)	AUC(%)	F1(%)	Acc(%)
Mean Pooling		✓		60.3	44.1	70.1	76.4	83.1	73.7
Max Pooling		✓		79.5	70.6	80.3	80.1	84.3	76.8
RNN-MIL [8]		✓		87.5	79.8	84.4	79.4	84.1	75.5
AB-MIL [8]		✓		85.4	78.0	84.5	81.2	86.0	78.1
DS-MIL [10]	✓	✓		89.9	81.5	85.6	86.1	86.6	81.4
CLAM-SB [14]		✓		87.1	77.5	83.7	82.1	84.3	77.1
CLAM-MB [14]		✓		87.8	77.4	82.3	81.7	83.7	76.3
TransMIL [18]		✓		90.6	79.7	85.8	81.2	84.4	76.7
DTFD-MIL [23]		✓		<u>93.2</u>	<u>84.9</u>	<u>89.0</u>	83.0	85.5	78.1
Ours (w/ Max Pooling)	✓	✓	✓	85.2 (+5.7)	74.7 (+4.1)	81.9 (+1.6)	86.6 (+6.5)	87.3 (+3.0)	82.0 (+5.2)
Ours (w/ AB-MIL)	✓	✓	✓	90.0 (+4.6)	80.5 (+2.5)	86.6 (+2.1)	87.1 (+5.9)	88.3 (+2.3)	83.3 (+5.2)
Ours (w/ DTFD-MIL)	✓	✓	✓	93.7 (+0.5)	87.0 (+2.1)	90.6 (+1.6)	87.7 (+4.7)	89.1 (+3.6)	83.5 (+5.4)

3.2 Implementation Details

For Camelyon16, we tile the WSIs into 256×256 patches on $20\times$ magnification using the official code of [23], while for the HCC dataset the patches are 384×384 on $40\times$ magnification following the pathologists' advice. For both datasets, we use an ImageNet pre-trained ResNet50⁷ to initialize $g(x)$ (except DS-MIL [10]). The instance embedding process is the same of [14], which means for each patch, it will be firstly embedded into a 1024-dimension vector, and then be projected to a 512-dimension hidden space for further bag-level training. For the training of bag classifier $f(x)$, we use an initial learning rate of $2e-4$ with Adam [9] optimizer for 200 epochs with batch size being 1. Camelyon16 results are reported on the official test split, while the HCC dataset uses a 7:1:2 split for training, validation and test. For the training of patch embedder $g(x)$, we use an initial learning rate of $1e-5$ with Adam [9] optimizer for 10000 iterations with batch size being 100. Three metrics are used for evaluation, namely area under curve (AUC), F1 score, and slide-level accuracy (Acc). Experiments are all conducted on a Nvidia Tesla M40 (12GB).

⁷ <https://download.pytorch.org/models/resnet50-11ad3fa6.pth>

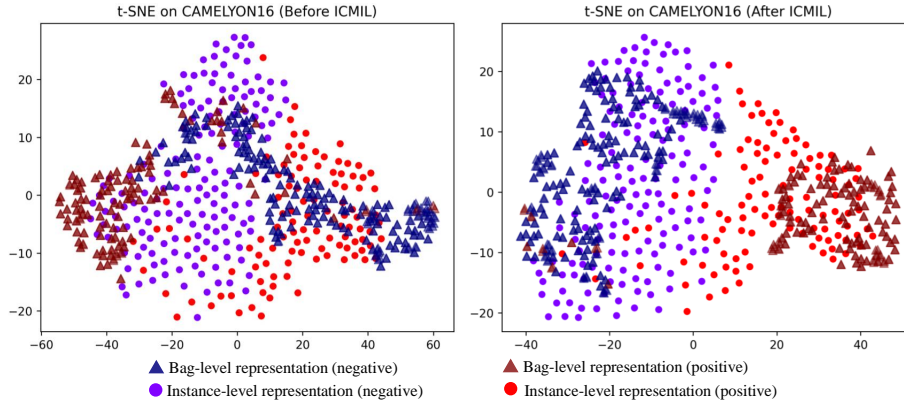


Fig. 5. Visualization of the instance- and bag-level representations before and after ICMIL training. Only one iteration of ICMIL is used to achieve the right figure.

3.3 Experimental Results

Ablation Study. The results of ablation studies are presented in Table 1. Please note that one complete ICMIL fine-tuning includes 1,000,000 randomly picked instances, and only after one complete iteration will the newly trained $f(x)$ be used as guidance for next iteration.

From Table 1(a), we can learn that as the number of ICMIL iteration increases, the performance will also go up until reaching a stable point. Since the number of instances is very large in WSI datasets, we finally choose to run ICMIL one iteration for fine-tuning $g(x)$ to achieve the balance between performance gain and time consumption. From Table 1(b), it is shown that our teacher-student based method outperforms the naïve ”pseudo label generation” method for fine-tuning $g(x)$, which proves the effectiveness of introducing the learnable instance-level classifier $f'(x)$.

Comparison with Other Methods. Experimental results are presented in Table 2. As shown, our ICMIL framework consistently improves the performance of three different MIL baselines (i.e., Max Pool, AB-MIL, and DTFD-MIL), demonstrating the effectiveness of bridging the loss back-propagation from bag classifier to embedder. It proves that a more suitable patch embedding can greatly enhance the overall MIL classification framework. When used with the state-of-the-art MIL method DTFD-MIL, ICMIL further increase its performance on Camelyon16 by 0.5% AUC, 2.1% F1, 1.6% Acc.

Results on the HCC dataset also proves the effectiveness of ICMIL, despite the minor difference on the relative performance of baseline methods. Mean Pooling performs better on this dataset due to the large area of tumor in the WSIs, which mitigates the impact of average pooling on instances. Also, the performance difference between different vanilla MIL methods tends to be smaller

on this dataset since risk grading is a harder task than Camelyon16’s identifying tumor cases. In this situation, the quality of instance representations plays a crucial role in generating more separable bag-level representations. As a result, after applying ICMIL on the MIL baselines, these methods all enjoy great performance boost on the HCC dataset.

Furthermore, Fig. 5 displays the instance- and bag-level representations of Camelyon16 dataset before and after applying ICMIL on AB-MIL backbone. The results indicate that one iteration of $g(x)$ fine-tuning in ICMIL significantly improves the instance-level representations, leading to a better aggregated bag-level representation naturally. Besides, the bag-level representations are also more closely aligned with the instance representations, proving that ICMIL can reduce the inconsistencies between $g(x)$ and $f(x)$ by coupling them together for training, resulting in a better separability.

4 Conclusion

In this work, we propose ICMIL, a novel framework that iteratively couples the feature extraction and bag classification steps to improve the accuracy of MIL models. Our proposed method bridges the loss propagation from bag classifier to patch embedder by leveraging the category knowledge in the bag classifier as pseudo supervision for embedder fine-tuning, and we also design a two-stream model to facilitate such knowledge transfer efficiently. The fine-tuned patch embedder can provide more accurate instance embeddings, in return benefiting the bag classifier. The experimental results show that our method brings consistent improvement to existing MIL backbones.

References

1. Bejnordi, B.E., Veta, M., Van Diest, P.J., Van Ginneken, B., Karssemeijer, N., Litjens, G., Van Der Laak, J.A., Hermesen, M., Manson, Q.F., Balkenhol, M., et al.: Diagnostic assessment of deep learning algorithms for detection of lymph node metastases in women with breast cancer. *Jama* **318**(22), 2199–2210 (2017)
2. Chen, Q., Xiao, H., Gu, Y., Weng, Z., Wei, L., Li, B., Liao, B., Li, J., Lin, J., Hei, M., et al.: Deep learning for evaluation of microvascular invasion in hepatocellular carcinoma from tumor areas of histology images. *Hepatology International* **16**(3), 590–602 (2022)
3. Chen, R.J., Chen, C., Li, Y., Chen, T.Y., Trister, A.D., Krishnan, R.G., Mahmood, F.: Scaling vision transformers to gigapixel images via hierarchical self-supervised learning. In: *Proceedings of the IEEE/CVF Conference on Computer Vision and Pattern Recognition*. pp. 16144–16155 (2022)
4. Cheng, N., Ren, Y., Zhou, J., Zhang, Y., Wang, D., Zhang, X., Chen, B., Liu, F., Lv, J., Cao, Q., et al.: Deep learning-based classification of hepatocellular nodular lesions on whole-slide histopathologic images. *Gastroenterology* **162**(7), 1948–1961 (2022)
5. He, K., Zhang, X., Ren, S., Sun, J.: Deep residual learning for image recognition. In: *Proceedings of the IEEE Conference on Computer Vision and Pattern Recognition*. pp. 770–778 (2016)

6. Hinton, G., Vinyals, O., Dean, J.: Distilling the knowledge in a neural network. arXiv preprint arXiv:1503.02531 (2015)
7. Hou, L., Samaras, D., Kurc, T.M., Gao, Y., Davis, J.E., Saltz, J.H.: Patch-based convolutional neural network for whole slide tissue image classification. In: Proceedings of the IEEE conference on computer vision and pattern recognition. pp. 2424–2433 (2016)
8. Ilse, M., Tomczak, J., Welling, M.: Attention-based deep multiple instance learning. In: International conference on machine learning. pp. 2127–2136. PMLR (2018)
9. Kingma, D.P., Ba, J.: Adam: A method for stochastic optimization. In: International Conference on Learning Representations (2015)
10. Li, B., Li, Y., Eliceiri, K.W.: Dual-stream multiple instance learning network for whole slide image classification with self-supervised contrastive learning. In: Proceedings of the IEEE/CVF conference on computer vision and pattern recognition. pp. 14318–14328 (2021)
11. Liu, K., Zhu, W., Shen, Y., Liu, S., Razavian, N., Geras, K.J., Fernandez-Granda, C.: Multiple instance learning via iterative self-paced supervised contrastive learning. arXiv preprint arXiv:2210.09452 (2022)
12. Lu, M., Pan, Y., Nie, D., Liu, F., Shi, F., Xia, Y., Shen, D.: Smile: Sparse-attention based multiple instance contrastive learning for glioma sub-type classification using pathological images. In: MICCAI Workshop on Computational Pathology. pp. 159–169. PMLR (2021)
13. Lu, M.Y., Chen, T.Y., Williamson, D.F., Zhao, M., Shady, M., Lipkova, J., Mahmood, F.: Ai-based pathology predicts origins for cancers of unknown primary. *Nature* **594**(7861), 106–110 (2021)
14. Lu, M.Y., Williamson, D.F., Chen, T.Y., Chen, R.J., Barbieri, M., Mahmood, F.: Data-efficient and weakly supervised computational pathology on whole-slide images. *Nature biomedical engineering* **5**(6), 555–570 (2021)
15. Luo, Z., Guillory, D., Shi, B., Ke, W., Wan, F., Darrell, T., Xu, H.: Weakly-supervised action localization with expectation-maximization multi-instance learning. In: Computer Vision—ECCV 2020: 16th European Conference, Glasgow, UK, August 23–28, 2020, Proceedings, Part XXIX 16. pp. 729–745. Springer (2020)
16. Maron, O., Lozano-Pérez, T.: A framework for multiple-instance learning. *Advances in neural information processing systems* **10** (1997)
17. Russakovsky, O., Deng, J., Su, H., Krause, J., Satheesh, S., Ma, S., Huang, Z., Karpathy, A., Khosla, A., Bernstein, M., et al.: Imagenet large scale visual recognition challenge. *International journal of computer vision* **115**(3), 211–252 (2015)
18. Shao, Z., Bian, H., Chen, Y., Wang, Y., Zhang, J., Ji, X., et al.: Transmil: Transformer based correlated multiple instance learning for whole slide image classification. *Advances in neural information processing systems* **34**, 2136–2147 (2021)
19. Srinidhi, C.L., Kim, S.W., Chen, F.D., Martel, A.L.: Self-supervised driven consistency training for annotation efficient histopathology image analysis. *Medical Image Analysis* **75**, 102256 (2022)
20. Wang, Q., Chechik, G., Sun, C., Shen, B.: Instance-level label propagation with multi-instance learning. In: Proceedings of the 26th International Joint Conference on Artificial Intelligence. pp. 2943–2949 (2017)
21. Wang, X., Tang, F., Chen, H., Luo, L., Tang, Z., Ran, A.R., Cheung, C.Y., Heng, P.A.: Ud-mil: uncertainty-driven deep multiple instance learning for oct image classification. *IEEE journal of biomedical and health informatics* **24**(12), 3431–3442 (2020)

22. Zhang, C., Song, Y., Zhang, D., Liu, S., Chen, M., Cai, W.: Whole slide image classification via iterative patch labelling. In: 2018 25th IEEE International Conference on Image Processing (ICIP). pp. 1408–1412. IEEE (2018)
23. Zhang, H., Meng, Y., Zhao, Y., Qiao, Y., Yang, X., Coupland, S.E., Zheng, Y.: Dtf-d-mil: Double-tier feature distillation multiple instance learning for histopathology whole slide image classification. In: Proceedings of the IEEE/CVF Conference on Computer Vision and Pattern Recognition. pp. 18802–18812 (2022)

Supplementary Materials

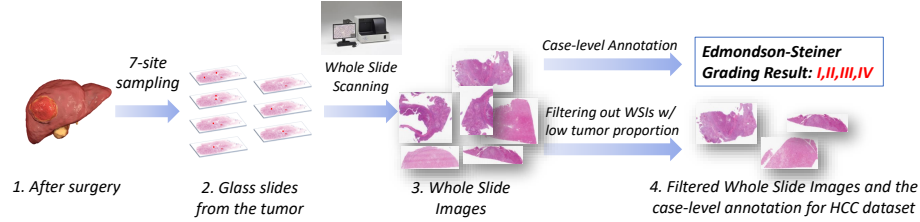


Fig. 6. The collecting process of the HCC dataset. We collect the HCC pathology dataset with a 7-site sampling procedure on the tumor tissues after surgery. Each annotation is provided by experienced pathologists based on the 7 WSIs of each case. However, to increase the training efficiency, we normally select 3 WSIs (sometimes 2 or 4 WSIs) with the highest tumor proportion in a case to form this HCC dataset. The 3 WSIs inherit the case-level label as their slide-level labels. In our experiments, WSIs with Edmondson-Stenier grading I, II are classified as low risk (negative in MIL), and III, IV are classified as high risk (positive in MIL).

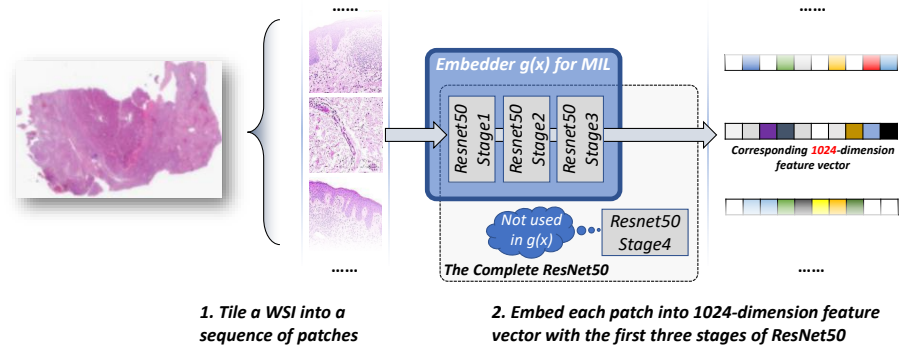


Fig. 7. Following previous works, we use the first 3 stages of ResNet50 for patch embedding, generating the 1024-dimension feature vectors for each patch as the final instance in the bag. The ResNet50 is initialized with ImageNet pre-trained weights, but is then finetuned in our proposed ICMIL to mitigate the domain shift for generating more optimal instance embeddings. It should be noted that ICMIL can also be used with other $g(x)$ structures to achieve similar effects.

Algorithm 1 Pseudo Code for ICMIL Training Pipeline

Input: WSI dataset X , annotations Y , loss function weight α , learning rate β_1, β_2 , and total ICMIL iteration times T

Output: Optimal MIL model components' weights $\theta^f, \theta^a, \theta^g$

- 1: **Initialize** θ^g with ImageNet pretrained weights for $g(x)$
- 2: **for** $iter$ **from** 0 **to** T **do** :
- 3: # Step 1: fix embedder $g(x)$ and train the bag classifier $f(x)$ ▷ Fig. 3(①)
- 4: **for** $x_i \in X$ **do** :
- 5: **for** $x_i^j \in Tiled(x_i)$ **do** :
- 6: $\hat{x}_i^j \leftarrow g(x_i^j)$
- 7: $\hat{x}_i \leftarrow \{\hat{x}_i^j | 0 \leq j \leq \text{len}(Tiled(x_i))\}$
- 8: $\hat{X} \leftarrow \{\hat{x}_i | 0 \leq i \leq \text{len}(X)\}$
- 9: $epoch \leftarrow 0$
- 10: **while** $epoch \leq 200$ **do** :
- 11: **for** $(\hat{x}_i, y_i) \in (\hat{X}, Y)$ **do** :
- 12: $l_{ce} \leftarrow \text{CrossEntropy}(\theta^a, \theta^f; f(a(\hat{x}_i)), y_i)$
- 13: $\theta^a = \theta^a - \beta_1 \nabla_{\theta^a}(l_{ce})$
- 14: $\theta^f = \theta^f - \beta_1 \nabla_{\theta^f}(l_{ce})$
- 15: $epoch \leftarrow epoch + 1$
- 16: **if** $iter = T$ **do**
- 17: **return** $\theta^f, \theta^a, \theta^g$
- 18: # Step 2: fix bag classifier $f(x)$ and finetune the embedder $g(x)$ ▷ Fig. 3(②)
- 19: $f'(\cdot) \leftarrow f(\cdot).copy()$ # Initialize an instance classifier $f'(\cdot)$ with $f(\cdot)$
- 20: $\theta^{f'} \leftarrow \theta^f.copy()$ # $f'(\cdot)$ use the same weights as $f(\cdot)$ initially
- 21: $g'(\cdot) \leftarrow g(\cdot).copy()$
- 22: $\theta^{g'} \leftarrow \theta^g.copy()$
- 23: $f(\cdot).require_grad \leftarrow \text{False}$
- 24: $g(\cdot).require_grad \leftarrow \text{False}$
- 25: **for** $x_i \in X$ **do** :
- 26: **for** $x_i^j \in Tiled(x_i)$ **do** :
- 27: $y_{teacher} \leftarrow f(g(x_i^j))$
- 28: $y_{student} \leftarrow f'(g'(Augment(x_i^j)))$
- 29: $l_c \leftarrow L_c(\theta^{g'}, \theta^{f'}; y_{student}, y_{teacher})$ ▷ Eqn. (3)
- 30: $l_w \leftarrow L_w(\theta^{f'}, \theta^f)$ ▷ Eqn. (4)
- 31: $l_{cw} = l_c + \alpha l_w$
- 32: $\theta^{f'} = \theta^{f'} - \beta_2 \nabla_{\theta^{f'}}(l_{cw})$
- 33: $\theta^{g'} = \theta^{g'} - \beta_2 \nabla_{\theta^{g'}}(l_{cw})$
- 34: $\theta^g \leftarrow \theta^{g'}.copy()$ # Update the embedder for next training iteration
